

Vibration-based structural health monitoring for offshore wind turbines – Experimental validation of stochastic subspace algorithms

Peter Kraemer^{*} and Herbert Friedmann^a

Wölfel Beratende Ingenieure GmbH + Co. KG, Max-Planck-Strasse 15, 97204 Höchberg, Germany

(Received December 3, 2015, Revised December 6, 2015, Accepted December 9, 2015)

Abstract. The efficiency of wind turbines (WT) is primarily reflected in their ability to generate electricity at any time. Downtimes of WTs due to “conventional” inspections are cost-intensive and undesirable for investors. For this reason, there is a need for structural health monitoring (SHM) systems, to enable service and maintenance on demand and to increase the inspection intervals. In general, monitoring increases the cost effectiveness of WTs. This publication concentrates on the application of two vibration-based SHM algorithms for stability and structural change monitoring of offshore WTs. Only data driven, output-only algorithms based on stochastic subspace identification (SSI) in time domain are considered. The centerpiece of this paper deals with the rough mathematical description of the dynamic behavior of offshore WTs and with the basic presentation of stochastic subspace-based algorithms and their application to these structures. Due to the early stage of the industrial application of SHM on offshore WT on the one side and the required confidentiality to the plant manufacturer and operator on the other side, up to now it is not possible to analyze different isolated structural damages resp. changes in a systematic manner, directly by means of in-situ measurement and to make these “acknowledgements” publicly available. For this reason, the sensitivity of the methods for monitoring purposes are demonstrated through their application on long time measurements from a 1:10 large scale test rig of an offshore WT under different conditions: undamaged, different levels of loosened bolt connections between tower parts, different levels of fouling, scouring and structure inclination. The limitation and further requirements for the approaches and their applicability on real foundations are discussed along the paper.

Keywords: offshore wind turbine; structural health monitoring; stochastic subspace identification

1. Introduction

In the past, different vibration-, guided waves- or acoustic-based SHM methods for offshore WTs were developed. To date no national or international standardizations or requirements for the SHM of WT by means of one method or another exists. In the industrial application, which this publication is focused on, mostly vibration-based, output-only methods are used. Data-driven methods are used for monitoring of damage and change detection (Link and Weiland 2014,

^{*}Corresponding author, Ph.D., E-mail: kraemer@woelfel.de

^a Ph.D., E-mail: friedmann@woelfel.de

Weijtjens *et al.* 2015, Kraemer 2011) and model-based methods for the life cycle estimation monitoring (Iliopoulos *et al.* 2016). Different methods for damage localization and damage extension are based on the analysis of local measurements (Link and Weiland 2014), however the model-based (e.g., finite element models) damage localization methods (Fritzen *et al.* 2010, Kraemer 2011) are currently not established for continuous monitoring purposes. Today, the localization and/or identification of damage resp. change type is possible only in a limited way by using different methods and indicators, where each method or indicator is more or less sensitive to one type of structural change or another (Link and Weiland 2014). An overall available algorithm, method or indicator for all kinds and types of WT structural damages does not exist. The selection of an algorithm resp. method depends on the monitoring purpose, structural hot spots, specifically on the dynamic behavior of the foundation and - not least - on the experience and knowledge of the SHM system designer on e.g., structural mechanics and dynamics, signal and data processing, statistical pattern recognition, big data handling, sensor selection, etc.

Further topics like sensor fault detection and compensation of environmental and operational conditions (EOCs) on the SHM-indicators are very important issues for the industrial application of SHM in harsh environments (Kraemer and Fritzen 2008). Only SHM-systems with self-diagnosis capability and the consideration of EOCs are really reliable and sensitive enough to detect damages and structural changes, insensitive to changes with EOCs and robust against sensor and hardware failures.

Actually, in offshore environment the sensors used for industrial SHM purposes measure mostly the acceleration, inclination, local strain or displacement of the WT structure in a low frequency domain (the wind and wave excitation occurs considerably below 10 Hz). In most of the cases the sensors are placed over the water level (Link and Weiland 2014, Kraemer and Fritzen 2010, Kraemer 2011). There are also a few instrumentations known with sensors under the waterline. However, the service life expectancy of those sensors is very low. The reliability/robustness of the communication between the components of the SHM-system like sensors, data acquisition units, data processing units, turbine controller, web interfaces for visualization and alarm management are very important and indispensable for a reliable SHM-system.

The basic principle of a vibration-based, output-only, data-driven SHM-method is illustrated in Fig. 1. The structural response at the sensor positions is measured (see block measurements in Fig. 1). The measured time series themselves are rarely directly used, but present meaningful features or feature vectors extracted from the signals that are useful to compare different structural states. The feature extraction is made by means of signal processing methods in time, frequency or time-frequency domain. Examples of features are statistical moments, characteristic numbers based on statistical moments, parameters of statistical distributions, coefficients of time series models, statistical characteristic numbers of time series residuals (e.g., from the “family” of autoregressive models), statistical characteristic numbers of stochastic model residuals, Fourier coefficients, frequencies obtained by spectral analysis, statistical moments of spectral data, eigenfrequencies, modal damping, mode shapes, modes curvatures calculated by means of operational modal analysis, wavelet coefficients, etc. The application of dynamic features in SHM-context is described in a compact form e.g., in Balageas *et. al.* (2006), Doebling *et al.* (1996), Fritzen and Kraemer (2009), Kraemer (2011).

The dynamic response and its features do not only contain the “isolated” system dynamics, but also effects of the EOCs on the structure and effects of the dynamic coupling on other parts of the turbine. So it is necessary that in a “learning phase”, the normal conditions of the structure under

different EOCs are identified and reference models for normal conditions are built (see block pattern recognition in Fig. 1). In the “detection phase”, the actual dynamic features of the structural parts are compared to the reference models. The residuals between the actual data and the reference models are statistically interpreted and “compressed” to one or more indicators (see block decision). In practice, different indicators calculated from signals of different sensors with their features and models are used and sometimes combined for monitoring of different structural parts. In this case each indicator has its sensitivity regarding different damages or changes. For the industrial application it is important, that the turbine operator (or directly the turbine controller) is provided with prompt and reliable decisions regarding the turbine state and necessary actions.

Some rough explanations of the WT dynamic behavior, feature extraction procedure, and reference model building for two stochastic subspace-based algorithms, along with formulas and figures are given in the following section.

2. Theoretical backgrounds – dynamic behavior of WT structures

The equations of a linear dynamic system already show that changes in stiffness and mass have an effect on the system's vibration behavior. This is one of the basic principles of the vibration-based damage identification approaches implemented in Wölfel's WT monitoring systems. The simple application of the linear and time-invariant equation of motion for the examination of a complex dynamic system on site (e.g. a wind turbine) is not sufficient.

The system is not stationary and superimposed by transient, stochastic and periodic excitations of the turbine. Due to variable boundary conditions, temperature fluctuations, changes of mass inertia moments, water level, etc., the dynamic system of a wind turbine is highly non-linear and can be well described by the following equations of motion (Balageas *et. al.* 2006, Fritzen *et al.* 2013a)

$$\mathbf{M}(\boldsymbol{\theta}_d, \boldsymbol{\theta}_e, \mathbf{x}, t) \ddot{\mathbf{x}} + \mathbf{g}(\boldsymbol{\theta}_d, \boldsymbol{\theta}_e, \mathbf{x}, \dot{\mathbf{x}}, t) = \mathbf{F}(\boldsymbol{\theta}_d, \boldsymbol{\theta}_e, t) \quad (1)$$

$$\dot{\boldsymbol{\theta}}_d = \mathbf{F}(\boldsymbol{\theta}_d, \boldsymbol{\theta}_e, \mathbf{x}, \dot{\mathbf{x}}, t) \quad (2)$$

$$\mathbf{y}(t) = \mathbf{h}(\boldsymbol{\theta}_d, \boldsymbol{\theta}_e, \mathbf{x}, \dot{\mathbf{x}}, t) \quad (3)$$

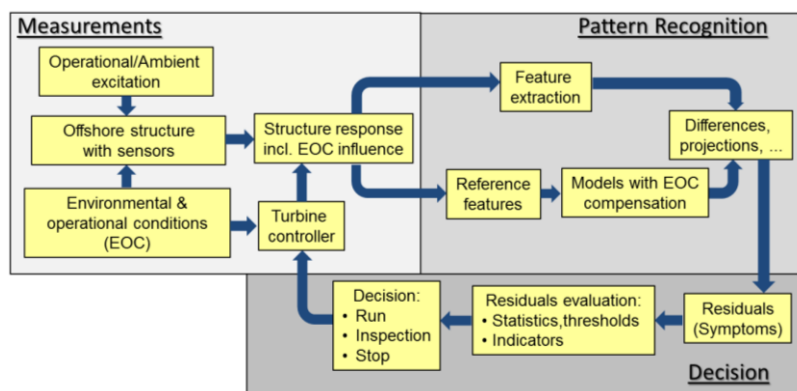


Fig. 1 Basic principle of a vibration-based, output-only, data-driven SHM-method

where \mathbf{M} is the mass matrix, \mathbf{g} the vector of elastic forces, damping forces, etc. and \mathbf{F} the external load vector; $\ddot{\mathbf{x}}$, $\dot{\mathbf{x}}$, \mathbf{x} are acceleration, velocity and displacement vectors. θ_d is a time (t) dependent vector with damage parameter, and the parameter vector θ_e indicates the influence of environmental and operational conditions, e.g. temperature, pitch angle, rotational speed, changing boundary conditions, etc. The non-linear function Γ describes the evolution of θ_d , e.g., crack length, play, loss of stiffness, change of mass, etc. A temporary decrease of system stiffness, e.g. as a result of damage, is formally assigned to θ_d , given that the damage is not one of the expected (normal) EOC changes. In the measurement Eq. (3), \mathbf{y} is the measured system response, which stays in a non-linear and time-variant relationship \mathbf{h} to $\theta_d, \theta_e, \mathbf{x}, \dot{\mathbf{x}}$ and t , see also Kraemer (2011).

As mentioned above, the measured data is not directly used to compare two system states. In fact, so-called features are extracted from the raw data, which are arranged in a vector. The feature vector \mathbf{f}_y extracted by the feature extraction operation (FE) is

$$\mathbf{f}_y(\theta_d, \theta_e) = FE(\mathbf{y}(\theta_d, \theta_e, t)) \quad (4)$$

The sensitivity of the i -th feature with respect to the j -th structural changes parameter is expressed by the first partial derivative

$$s_j = \frac{\partial f_y(\theta_d, \theta_e)}{\partial \theta_{dj}} \quad (5)$$

and shows that the dynamic behavior of the structure and its features depend simultaneously on damage state and the EOC. Thus, the compensation of the effect of EOCs on the dynamic behavior of a wind turbine is of particular importance.

3. Structural change detection based on stochastic subspace algorithms

Two vibration-based SHM-algorithms appropriate for stability and structural change monitoring of offshore wind turbines are presented below, both of them belonging to the stochastic subspace identification (SSI). The first approach considers only changes of lower order stochastic subspace models, which can be interpreted in a physical way as changes in the vibration modes. This is based on the covariance-driven stochastic subspace identification (SSI-COV) algorithm and often is used in context of operational modal analysis (Van Overschee and De Moor 1996, Peeters and De Roeck 1999). The second method, however, also considers the changes in the higher orders of stochastic models and is known (Basseville *et al.* 2000) as the stochastic subspace fault detection (SSFD) algorithm or null space-based fault detection algorithm (NSFD). Since the purpose of this publication is to show the sensitivity of the approaches due to structural changes of offshore WT, the aspects of EOC compensation on the extracted features are only briefly sketched (specific information about EOC compensation can be found e.g., in Fritzen *et al.* 2013a, b).

3.1 SSI-COV-based structural change detection

As features of the dynamic system the eigenmodes are calculated and automatically interpreted

in the following steps. First, the non-linear Eq. (1) is fragmented by several linear, time-invariant equations, with unknown stochastic input, each only available for different classes of EOCs. The criteria for choosing class ranges and number of classes are defined by means of Eq. (5). The state space representation of one equation for one EOC class e is

$$\begin{aligned} (\mathbf{z}_{k+1})_e &= (\mathbf{A}_d)_e \mathbf{z}_k + \mathbf{w}_k \\ (\mathbf{y}_k)_e &= \mathbf{C}_y (\mathbf{z}_k)_e + \mathbf{v}_k \end{aligned} \quad (6)$$

where \mathbf{z} is the state vector and \mathbf{y} contains the multivariate time data of the measured sensor signals, \mathbf{A}_d is the discrete state space matrix, \mathbf{C}_y is the measurement matrix, \mathbf{w} and \mathbf{v} are the process and measurement noise respectively, k is one time instant in the measured signals.

It is well known that matrix \mathbf{A}_d is a function f of the auto- and cross-correlation function of the measured time series \mathbf{y} (of length n_t)

$$\hat{\mathbf{R}}_r = \frac{1}{n_t - r - 1} \sum_{k=1}^{n_t - r} \mathbf{y}_{k+r} \mathbf{y}_k^T \quad (7)$$

e.g., arranged in a matrix with Hankel-Canonical form \mathbf{H}

$$(\mathbf{H}_{\alpha,\beta})_{r-1} = \begin{bmatrix} \hat{\mathbf{R}}_r & \hat{\mathbf{R}}_{r+1} & \cdots & \hat{\mathbf{R}}_{r+\beta-1} \\ \hat{\mathbf{R}}_{r+1} & \hat{\mathbf{R}}_{r+2} & \cdots & \hat{\mathbf{R}}_{r+\beta} \\ \vdots & \vdots & \ddots & \vdots \\ \hat{\mathbf{R}}_{r+\alpha-1} & \cdots & \cdots & \hat{\mathbf{R}}_{r+\alpha+\beta-2} \end{bmatrix} \quad (8)$$

For $r = 1$ the Hankel matrix can be expressed as the product of the observability and controllability matrix with the time shifts α , β respectively. The identification of the reduced system of order p follows by the singular value decomposition (SVD) of the Hankel matrix $\mathbf{H}_0 \approx \mathbf{U}_p \mathbf{S}_p \mathbf{V}_p^T$ for $r = 1$

$$\hat{\mathbf{A}}_d = \mathbf{S}_p^{-1/2} \mathbf{U}_p^T \mathbf{H}_1 \mathbf{V}_p \mathbf{S}_p^{-1/2} \quad (9)$$

In the second step the eigenfrequencies of the system and the modal damping ratios for one EOC-combination e are identified by means of the state space matrix eigenvalues. Multiplying the eigenvectors of $\hat{\mathbf{A}}_d$ by the system output matrix $\hat{\mathbf{C}}_y = \mathbf{E}^T \mathbf{U}_p \mathbf{S}_p^{1/2}$ (with $\mathbf{E}^T = [\mathbf{I} \ \mathbf{0} \ \cdots \ \mathbf{0}]$) provides the complex mode shapes of the system.

The third step consists in the automated selection of stable poles from stability plots. Such a stability plot gained from measured data of a wind turbine structure is shown in Fig. 2(a). The black circles indicate that the eigenfrequencies, the modal damping and the mode shapes do not change with higher model (state space) order. The continuous gray line represents the mean power spectral density (PSD) of the signals; this line has no meaning for the feature extraction and just shows that the stable frequencies are close to the peaks of PSD. Only using stability plots is not enough for an automatic feature extraction approach. For this purpose, further classification algorithms are used. These algorithms automatically choose the number of class centers and give the representative stable poles at the class centers (see the blue vertical straight lines in Fig. 2(a)).

After these steps, the sensitivities of the modal parameters due to the changes of EOCs are well known and can be modeled by means of linear or non-linear correlations. Fig. 2(b) shows the linear dependency of one eigenfrequency on the temperature. Of course, depending on the vibration mode, the feature vector (modal data) shows different dependencies to different EOCs (not shown here). The impact of the EOCs on the modal data is shown by Eq. (5). These dependencies/models are established during the time when there is no structural change of the WT (“learning phase”). These models represent the system references.

If the actual feature vector (during the “detection phase”) shows a significant statistical deviation from the reference in (%), an alarm is triggered. The state condition of the plant is summarized in just one indicator/ residual, which is proportional to the structural changes.

3.2 NSFD based structural change detection

An alternative indicator based on residuals generated by means of the Hankel-matrices left kernel space was first proposed in (Basseville *et al.* 2000). This residual turned out to be very sensitive to small structural changes. The column vectors of the matrix of left singular vectors obtained from SVD: $\mathbf{U}_p = \mathbf{K}^T$ span the null space (or left kernel space) of the reduced Hankel matrix of the undamaged structure with $\mathbf{H}_{ref} = (\mathbf{H}_{\alpha,\beta})_0$ so that

$$\mathbf{K}_{ref} \mathbf{H}_{ref} = \mathbf{0} \quad (10)$$

will be used to generate the residuals from the incoming data sets (index n) $\boldsymbol{\varepsilon}_n = \mathbf{K}_{ref} \mathbf{H}_n$ which can be compressed to one damage indicator/residual

$$\chi_n^2 = \boldsymbol{\zeta}_n^T \hat{\Sigma}^{-1} \boldsymbol{\zeta}_n \text{ with } \boldsymbol{\zeta}_n = \text{vec}(\boldsymbol{\varepsilon}_n) \text{ and } \hat{\Sigma} = \frac{1}{N_\Sigma - 2} \sum_{q=2}^{N_\Sigma} \boldsymbol{\zeta}_q \boldsymbol{\zeta}_q^T. \quad (11)$$

vec in Eq. (11) is the one vector stack operator and N_Σ is a number of data sets belonging to the undamaged structure used to define the covariance matrix $\hat{\Sigma}$. Details of the algorithm can be found in Balageas *et al.* (2006).

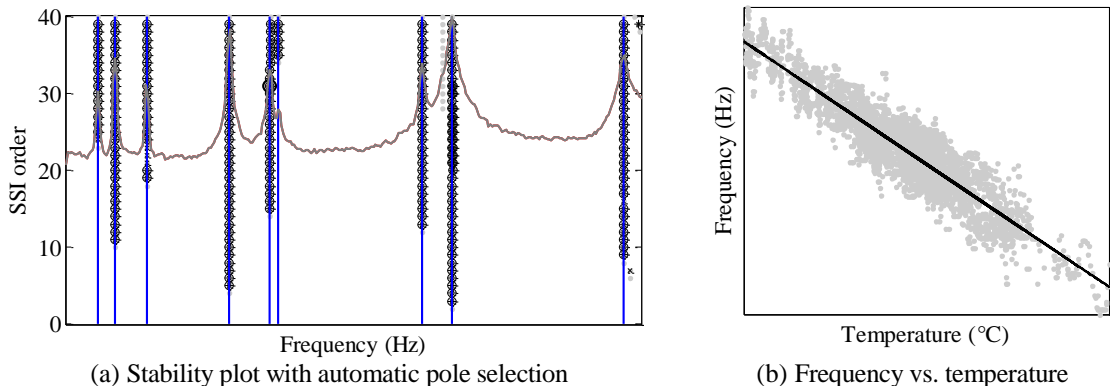


Fig. 2 Features and EOC-compensation within SSI-COV-based method

4. Experimental validation

As already mentioned, it is not possible to analyze different isolated structural damages or changes in a systematic manner, directly by means of in-situ measurements on existing WTs. For this reason, the sensitivity of the methods for monitoring purposes are demonstrated through their application on a long time measurement campaign at a 1:10 large scale test rig of an offshore WT. These examinations were done during the R&D-project *UnderwaterINSPECT* funded by the German Federal Ministry for Economic Affairs and Energy.

4.1 Test rig, test facilities and experiment purposes

The test rig consisted of a model of the WT structure with monopile foundation placed in the test hall and the sand basin of Test Center for Support Structures of Leibniz Universität Hannover, see Fig. 3(a). The measurements were done together with Fraunhofer IWES. The dimensions of the test pit were 10x14x10 m. The pit was filled with sand and water. The water level was controlled.

The monopile structure, see Fig. 3(b), consisted of two pipes of approx. 0.5 m of diameter and approx. 6 mm of wall thickness. The length of the first pipe (pile model) was 7.5 m. This was vibrated into the sand for a depth of 6 m. The second pipe (tower model) was flanged by means of 20 screws to the first one and had a length of 6.5 m. At the top of the “tower” an electro-magnetic shaker was mounted. The shaker represented the turbine and excited the structure by means of stochastic forces.

Different sensors for different purposes were installed on the structure; some of the sensors were applied on the first pipe (in the sand), the other sensors on the second pipe. The sensor types and positions can be seen in Fig. 4. For the validation of SSI-COV- and NSFD-based methods only the acceleration signals (the sensors are placed over the “water level”) were used. The used frequency range from the acceleration signals was 0-125 Hz. The frequency range of the stochastic excitation by the shaker was between 2-50 Hz, the forces were assumed to be unknown. The measurement time for each data set displayed in the following graphics was 10 minutes.

The experiment aimed at the validation and development of different approaches for WT monitoring. In this publication, the testing and validation of the sensitivity of two stochastic subspace-based change-detection approaches regarding:

- soil degradation,
- loosened bolts at the flange (represents a loss of stiffness),
- fouling (additional masses),
- scouring (changing of boundary conditions) and
- structure inclination.

is described.

4.2 Results of soil degradation

The first tests were made with a shaker excitation of 350 N (RMS value). During this excitation and without any structural changes the first eigenfrequency (approx. 4.3 Hz) of the monopile changed significantly, see Fig. 5. The reason was the high excitation level, which led to soil

loosening. Perhaps this phenomenon was caused by pile driving during its vibration into the soil. In reality, if the foundation is rammed by hammer impact a soil hardening is expected within the first weeks after the WT installation.

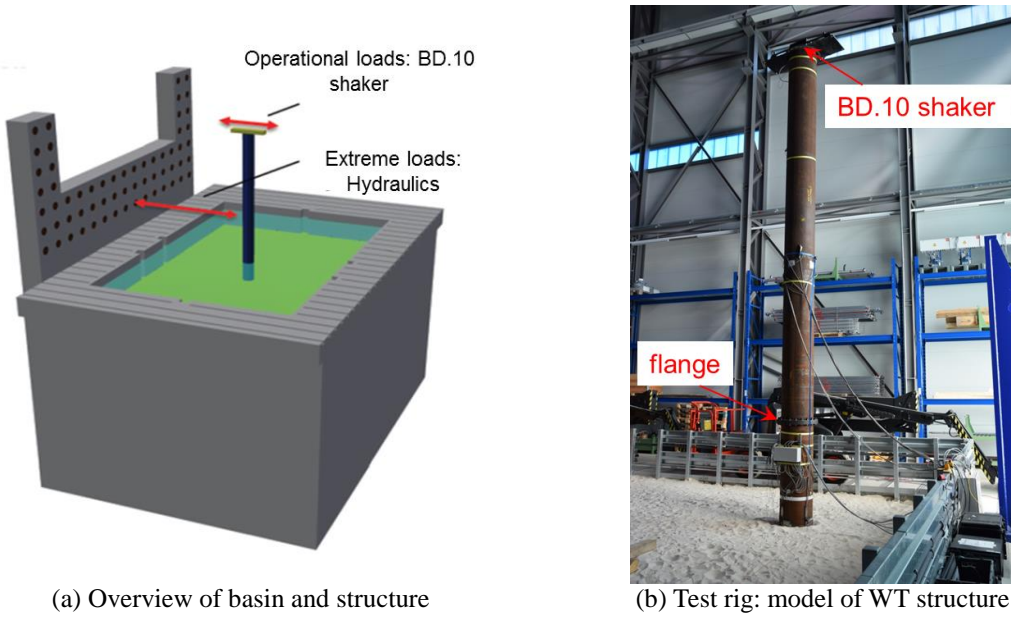


Fig. 3 Test rig in the sand basin of Test Center for Support Structures

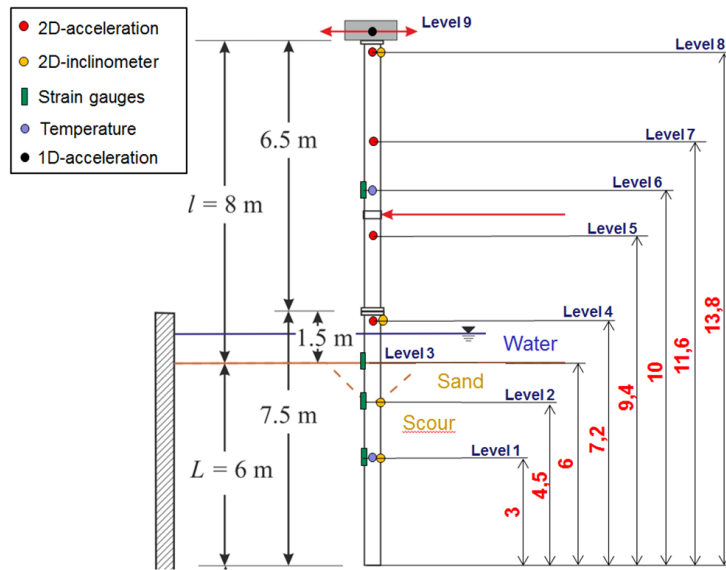


Fig. 4 Dimensions and instrumentation of the structure

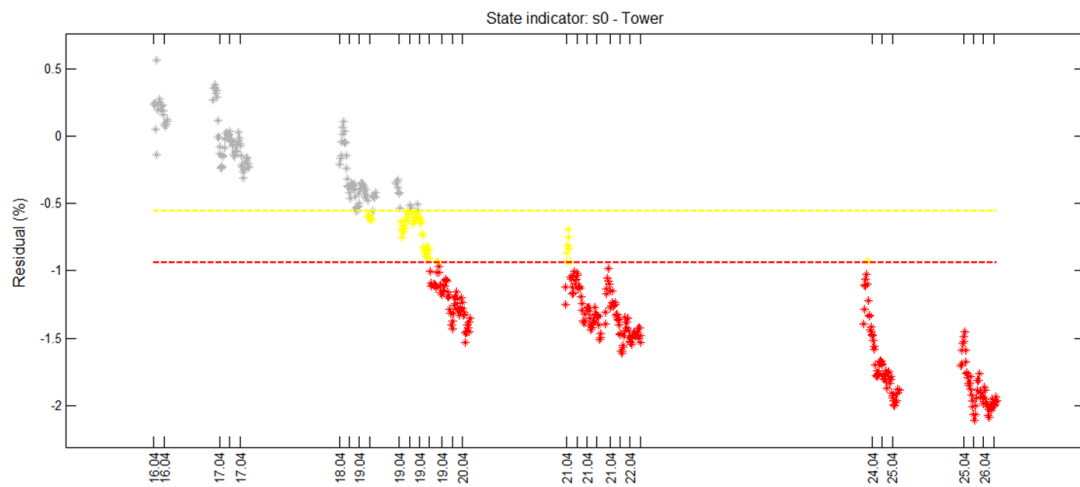


Fig. 5 Change of first eigenfrequency due to “soil degradation”

Under this condition it was evident that effects of induced damages, etc. would be covered up by those of soil changes. For this reason the excitation level by the shaker was reduced to 250 N (RMS). With this condition the soil degradation was much slower than before.

The time-history of all the measurements during different structural changes and their effect on the first eigenfrequency are shown in Fig. 6.

For overview reasons in the next graphics the measurement number (instead of the measurement date) will be assigned to the x-axis.

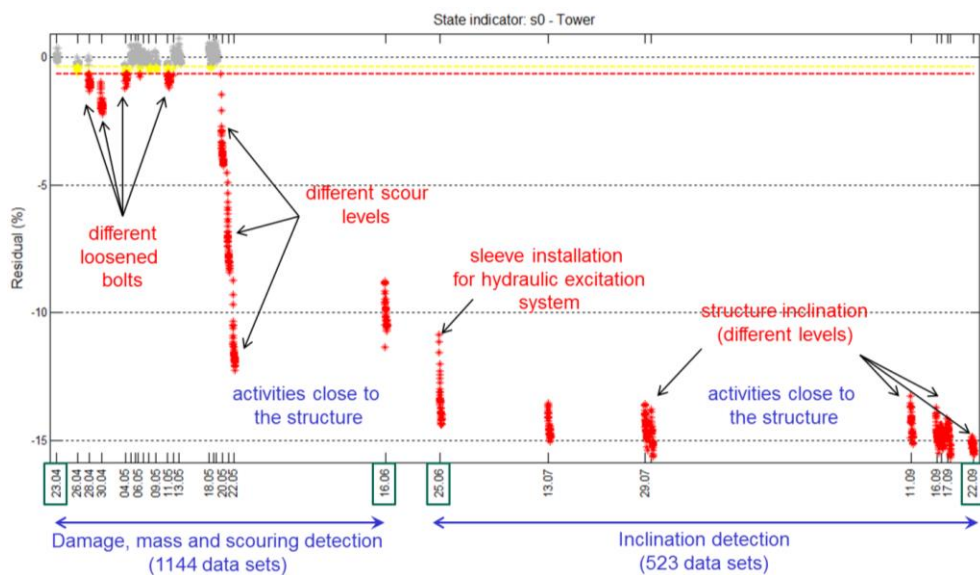


Fig. 6 Measurement plan and change of first eigenfrequency during all measurements

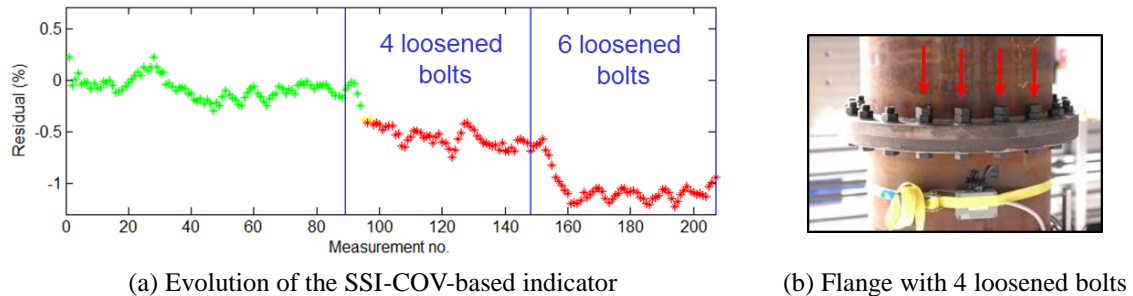


Fig. 7 Effects of loosened bolts at the flange

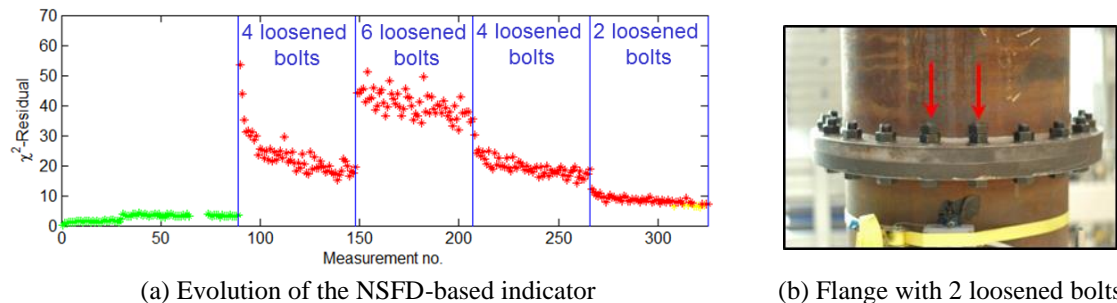


Fig. 8 Effects of loosened bolts at the flange

4.3 Loosened bolts at the flange

Different damage levels were created by the loosening of 2, 4 or 6 of the flange connection bolts between pile and tower (the flange connection consists of 20 bolts). For security reasons the bolts were not completely loosened, a rest tension remained in the bolts, these were additionally secured by means of counter nuts, as seen in Figs. 7(b) and 8(b).

The method based on the eigenfrequencies change (four simultaneous eigenfrequencies), showed that 4 and 6 loosened bolts could be well detected, see Fig. 7(a), also the detection of 2 loosened bolts was possible in a limited way (the results are not shown here since a very clear and distinct difference between the reference state and 2 loosened bolts was not significant).

The NSFD-based method clearly shows that all levels of loosened bolts can be well identified, see Fig. 8(a).

4.4 Fouling simulation by means of additional masses

The fouling could be only simulated in a very simplified way by placing additional masses close to the flange. Three different additional masses were mounted to the tower: 4, 20 and 30 kg, as displayed in Fig. 9(b). The mass of the tower and shaker was approx. one ton.

The NSFD-based method was able to detect the changes due to additional masses, see Fig. 9(a), the SSI-COV-based method was not suitable for clear detection of those masses. Since fouling belongs to the “normal” states of the structure, if its effect on the NSFD-indicators is not

compensated, this can cover up the effects of small damages e.g., as the loosening of 2 bolts (the NSFD-indicator is in both cases: 2 loosened bolts and 4 kg additional mass relative similar, approx. 10, compare Fig. 9(a) to Fig. 8(a)).

4.5 Scouring

Scouring are changes between the structure and the surrounding soil, affecting the structural stability. Also different scouring levels were simulated by grubbing out 30, 60 and 80 cm of sand around the structure.

The effects of scouring on the indicators of both methods are huge, see Fig. 10(a) for SSI-COV-based method and Fig. 11 for NSDF-based method. So it can be supposed, that if scouring is treated simultaneously to other effects e.g. coming from loose of stiffness (damages) the effect of scouring will be dominant and possibly cover up all other effects. In this case it is important for the mentioned change resp. damage detection procedures either to build the references after the scour depth is no longer growing (some months after WT installation) or to compensate the scour effects on the indicators. The first option is dangerous, since during strong storms the scour can change again. The last option is possible if the scour depth is measured by means of other sensors (e.g., sonar).

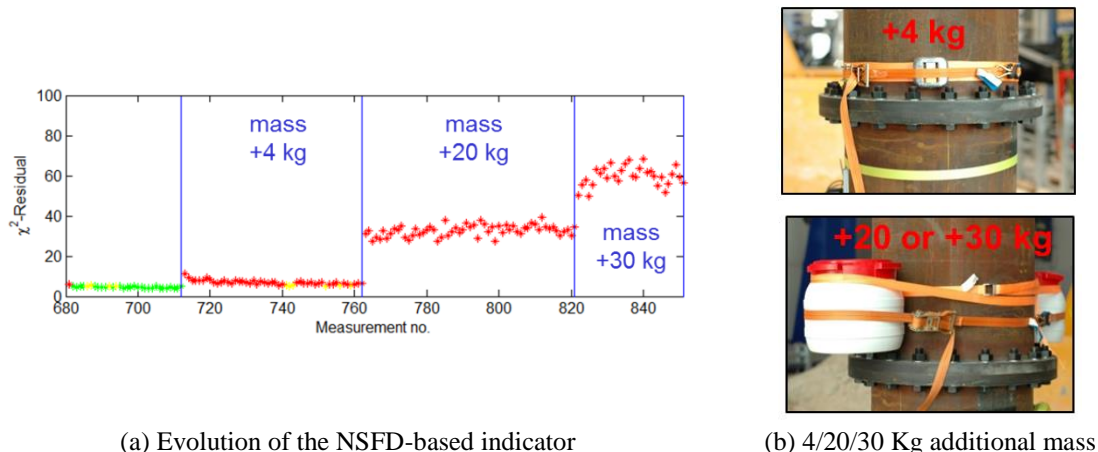


Fig. 9 Effects of additional masses positioned over the flange

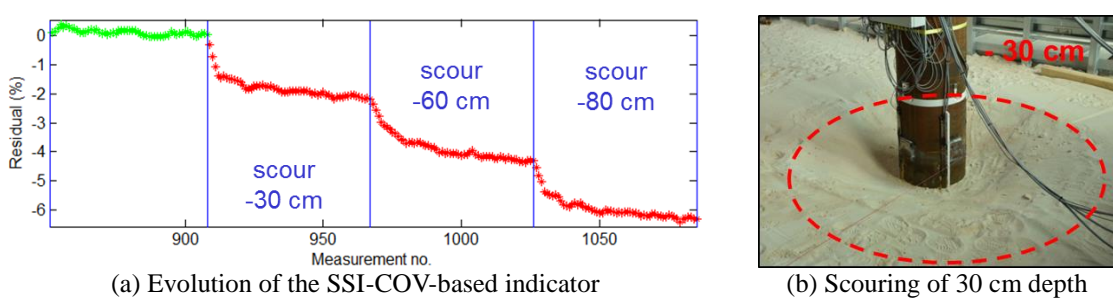


Fig. 10 Effects of scouring

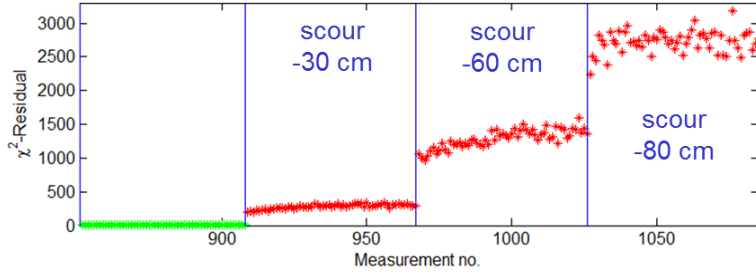
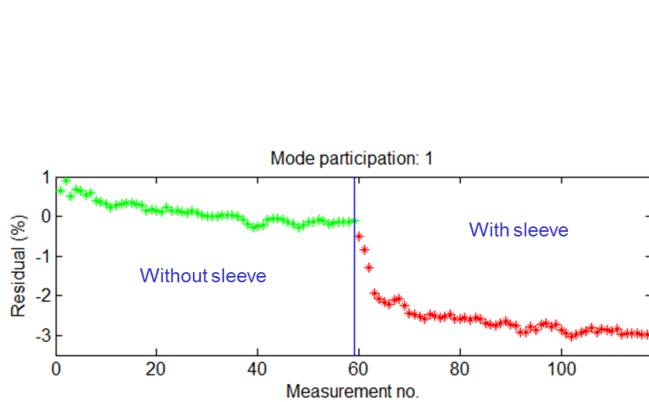


Fig. 11 Evolution of the NSFD-based indicator

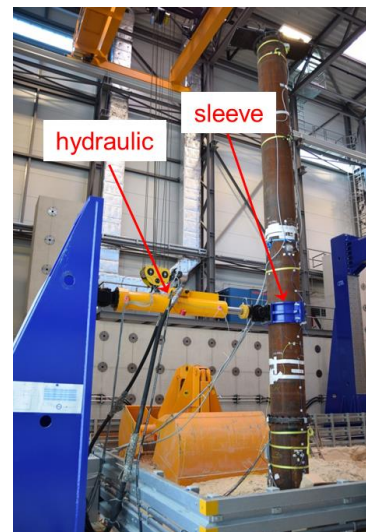
4.6 Structure inclination

The structure inclination was reached by means of periodic eccentric loads from a hydraulic cylinder. The hydraulic system was coupled to the tower through a sleeve (weight: approx. 50 kg), as shown in Fig. 12(b). The effect of sleeve mounting (without hydraulic coupling) on the structure first eigenfrequency is shown in Fig. 12(a).

Some measurements with the hydraulic system acting (loading period) on the structure are shown in Fig. 13. Depending on the eccentric loads, different levels of structure inclination at tower top were reached (see L1:L4 in Fig. 13). The remaining inclination after each loading period is smaller than 0.05° . After each loading period the hydraulic system was decoupled (but the sleeve still remained on the structure) and the structural response during the shaker excitation was measured (as already described in 4.1).



(a) Evolution of the first eigenfrequency



(b) Structure with sleeve and hydraulic

Fig. 12 Hydraulic installation for eccentric loading of the structure

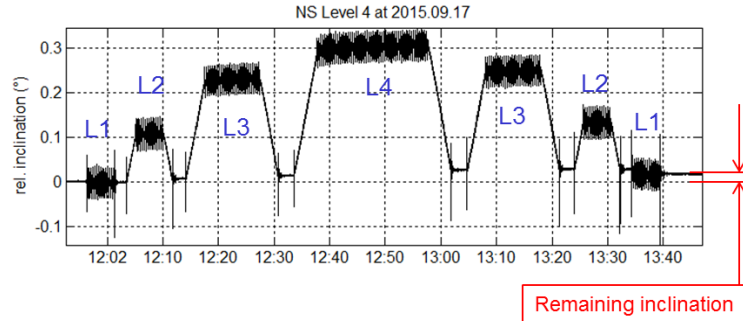


Fig. 13 Tower top inclination during loads from hydraulic

The lower part of Fig. 14 shows that after each hydraulic loading the remaining inclination was higher than at the previous hydraulic loading. During the shaker excitation the structure was gradually straightened. Both, the hydraulic loading and the excitation by the shaker led to the structure soil connection changes. The simultaneous effects of the soil structure connection changes and structure inclination can be seen in the changes of the first eigenfrequency of the structure (upper part of Fig. 14). Here it is impossible to separate these effects by means of one of the methods based on stochastic subspace identification. In the case of structure inclination monitoring it is more useful to use directly the information from the inclination measurements.

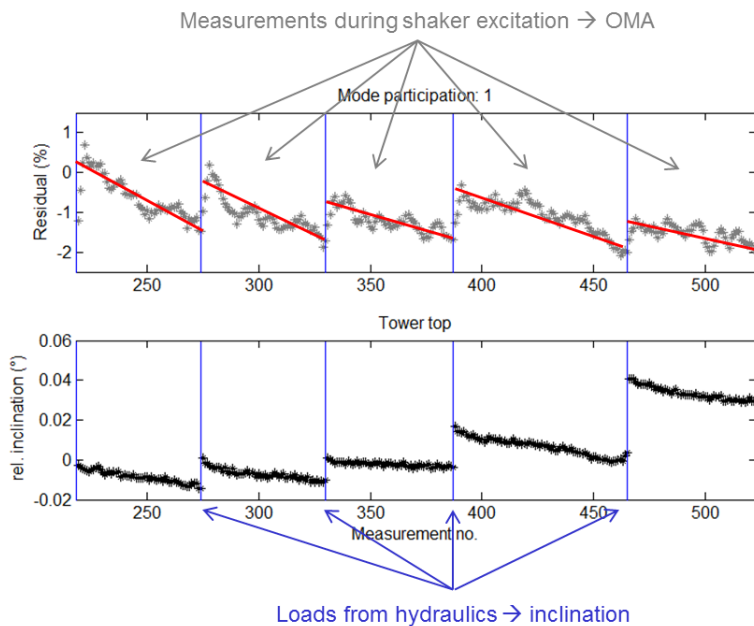


Fig. 14 Structure inclination after hydraulic loading and during shaker excitation

5. Conclusions

The sensitivity and limitation of two stochastic subspace identification methods for SHM of foundations of WTs were investigated by means of a long-time measurement campaign. The measurement was performed at a 1:10 large-scale test rig of an offshore WT under different conditions: no damage, structural changes, different levels of loosened bolt connections between pile and tower, different levels of fouling, scouring and structure inclination.

The results show that both methods are sensitive to small damages as loosened bolts in the flange connections and also to changes in the system stability induced by scouring. The NSFD-based method is sensitive to mass changes too. The essential knowledge or lesson learned from the application of the methods on the measured data at the test rig is: In general, the approaches are more sensitive to soil changes than to structural changes. Based on this knowledge, if the structural change detection of a WT has to be monitored in presence of strong soil changes, the effects of soil changes have to be compensated, e.g., by means of separate scour depth measurements (options for compensation of measured parameters on stochastic subspace indicators are already available and can be found in Kraemer 2011 and Fritzen *et al.* 2013b).

Further collected data during the test rig measurements will be used to validate available mathematical data-driven methods (e.g. based on vector autoregressive models, further statistical models in time or time-frequency domain) and to design the structural-model-based approaches in a reliable manner for the purposes of damage localization and remaining life-cycle estimation (only with few sensors installed on the tower, over the water level).

Effects of grout damages will be examined during a second R+D-project, QS-M Grout, which has already started.

Acknowledgments

The authors are grateful to the German Federal Ministry for Economic Affairs and Energy for the financial support of *UnderwaterINSPECT* project (grant no. FKZ 03SX345A) and to the Fraunhofer IWES for their support and the excellent cooperation during the measurement campaign at the Test Center for Support Structures.

References

- Balageas, D., Fritzen, C.P. and Güemes, A. (2006), *Structural Health Monitoring*, Hermes Science Publishing.
- Basseeville, M., Abdelghani, M. and Benveniste, A. (2000), "Subspace-based fault detection algorithms for vibration monitoring", *Automatica*, **36**, 101-109.
- Doebling, S.W., Farrar, C.R., Prime, M.B. and Shevitz, D.W. (1996), *Damage Identification and Health Monitoring of Structural and Mechanical Systems from Changes in Their Vibration Characteristics: A Literature Review*, Report LA-13070-MS, Los Alamos, USA.
- Fritzen, C.P., Klinkov, M. and Kraemer, P. (2013a), "Vibration-based damage diagnosis and monitoring of external load", *New Trend. Struct. Health Monit.*, **542**, Springer.
- Fritzen, C.P., Kraemer, P. and Büthe, I. (2013b), "Vibration-based damage detection under changing environmental and operational conditions", *Adv. Sci. Technol.*, **83**, 95-104.
- Fritzen, C.P. and Kraemer, P. (2009), "Self-diagnosis of smart structures based on dynamical properties",

- Mech. Syst. Signal Pr.*, **23**, 1830-1845.
- Fritzen, C.P., Kraemer, P. and Klinkov, M. (2010), "Schwingungsbasierte Schadensdiagnose für Offshore-Windenergieanlagen", *Proceedings of the Schwingungsanalyse & Identifikation*, Leonberg, Germany.
- Iliopoulos, A., Shirzadeh, R., Weijtjens, W., Guillaume, P., Van Hemelrijck, D. and Devriendt, C. (2016), "A modal decomposition and expansion approach for prediction of dynamic responses on a monopile offshore wind turbine using a limited number of vibration sensors", to be published in *Mech. Syst. Signal Pr.*, **68-69**, 84-104.
- Kraemer, P. (2011), *Damage diagnosis approaches for structural health and condition monitoring of offshore wind energy plants*, PhD Thesis, University of Siegen.
- Kraemer, P. and Fritzen, C.P. (2008), "Sensor fault detection and signal reconstruction using mutual information and Kalman filters", *Proceedings of the International Conference on Noise and Vibration Engineering*, Leuven, Belgium.
- Kraemer, P. and Fritzen, C.P. (2010), "Aspects of operational modal analysis for structures of offshore wind energy plants", *Struct. Dynam. Renew. Energy*, 145-152.
- Link, M. and Weiland, M. (2014), "Structural health monitoring of the monopile foundation structure of an offshore wind turbine", *Proceedings of the EURODYN 2014*, Porto, Portugal.
- Peeters, B. and De Roeck, G. (1999), "Reference-based stochastic subspace identification for output-only modal analysis", *Mech. Syst. Signal Pr.*, **12**(6), 855-878.
- Van Overschee P. and De Moor, B. (1996), *Subspace Identification for Linear Systems, Theory, Implementation, Applications*, Kluwer Academic Publishers.
- Weijtjens, W., Verbelen, T., De Sitter, G. and Devriendt, C. (2015), "Foundation structural health monitoring of an offshore wind turbine - a full-scale case study", *Struct. Health Monit.*, 1-14.

